The case study presented herein is a simply supported beam design according to ACI-318-08 with a span of 2.2 m, with dimensions 150mm wide and 250mm deep. The beam is reinforced with 2 Nos. of 12mm diameter high yield bars as main longitudinal reinforcement and 8mm shear links at 100mm spacing. The details of the beam are shown in Fig 1. A finite element model of the beam was created using 20-node brick elements to represent the concrete while the reinforcement was modelled with 2-node embedded bar elements inside 3-D brick elements, Fig. 2. Initially Eigen value analysis of the undamaged beam was performed, and the mode shape vectors were obtained. Subsequently non-linear static analysis was carried out for two different applied load conditions namely up to 50% and 70% of the ultimate load in order to induce damage in the beam. For the case when the load was applied at 0.5L, ultimate load was 45 kN, such that 50% and 70% are 23kN and 32.2kN, respectively. Correspondingly when applied load was at 0.25L, the ultimate load was 56kN, giving the 50% and 70% values of 28kN and 39.2kN. After each of the applied load condition, the load was released, and Eigen value analysis was again carried out to obtain the mode shape vectors for the damaged beam. Different locations of damage in the beam were achieved by applying the concentrated point load at mid-span and quarter span points along the beam. Fig. 3 shows the crack pattern in the RC beam after application of the damage load.

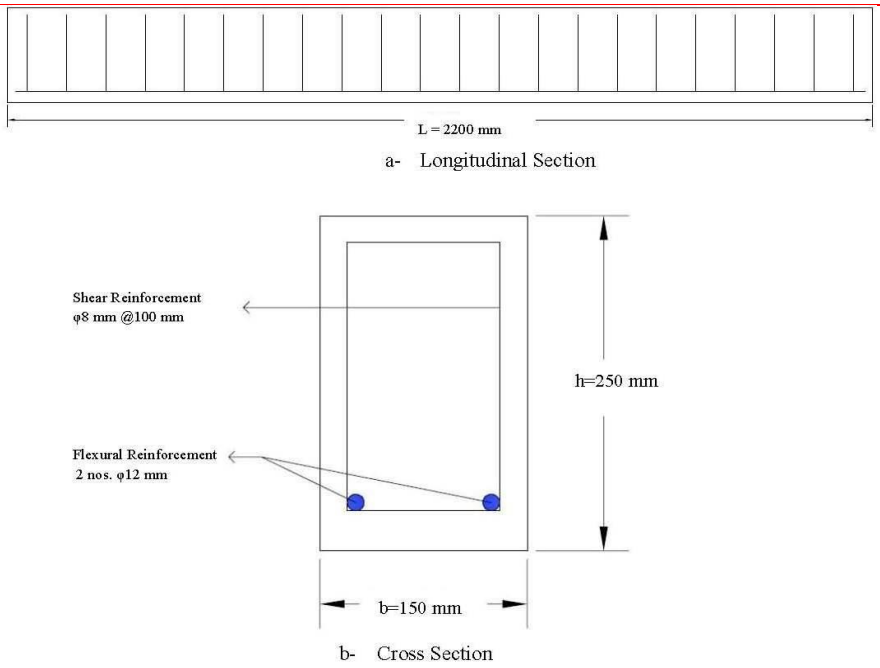

Fig. 1 Reinforced concrete beam dimensions and details

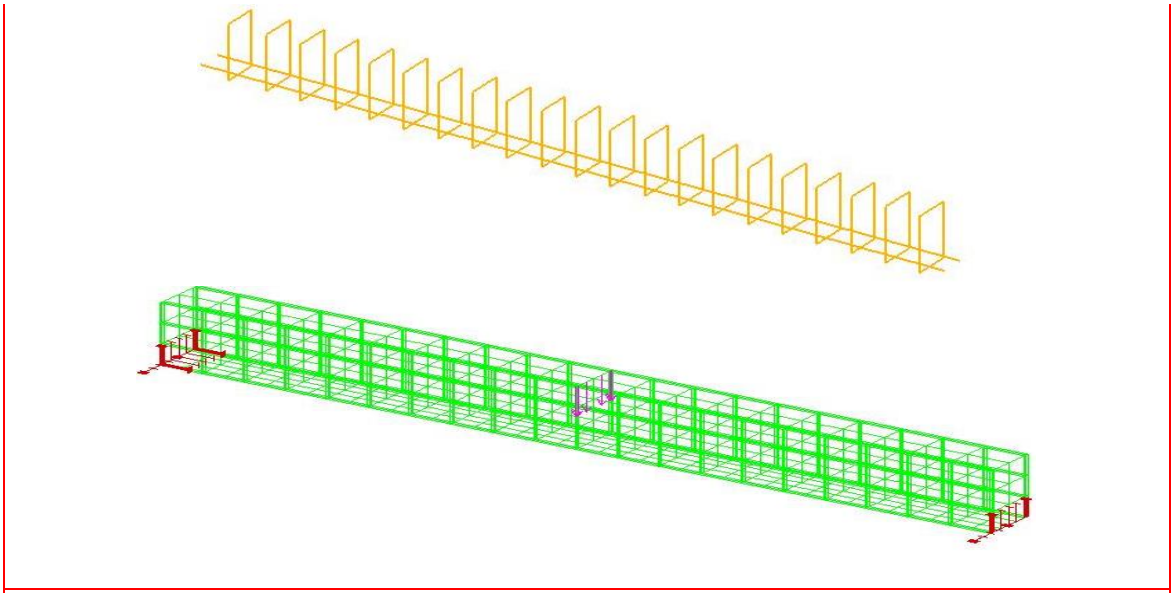

Fig. 2 Finite element model of reinforced concrete beam (top: reinforced bars modelling; bottom: concrete beam modelling)

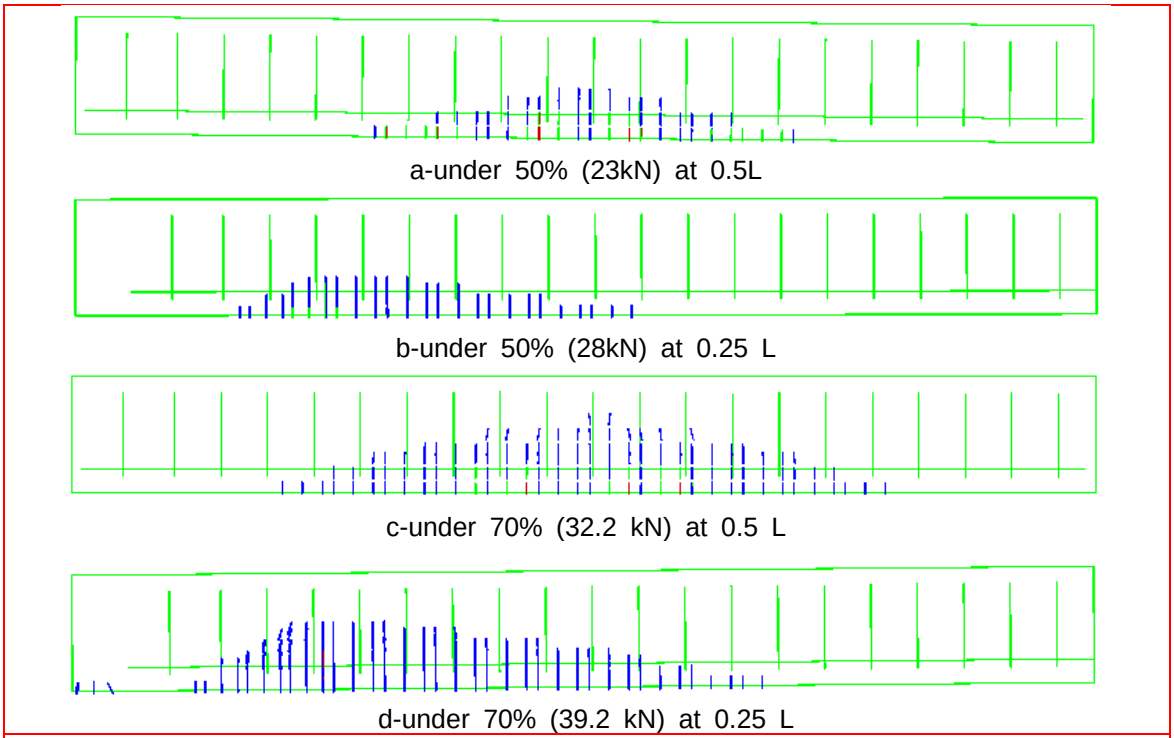

Fig. 3 Crack pattern of RC beam under different damage load located at different distance from left support (Cracks are shown in blue and red)

3. Damage detection algorithms

The results obtained from the finite element analysis were subsequently utilized to verify and compare the sensitivity and accuracy to detect and locate the damage positions, respectively in this study. The eigenvectors were substituted into the equations for the damage algorithms namely the Curvature Damage Factor (CDF) and Local Stiffness Indicator (LSI).

3.1 Curvature Damage Factor CDF

Proposed by Wahab and De Roeck (1999), the mode shape curvature at each point is computed from central difference approximation using mode displacement as given in Eq. (1) below.

$$Ci = (y_{i+1} - 2y_i + y_{i-1})/h^2 \quad (1)$$

where C is the curvature, i is node number, y is the Eigen vector at ith node, and h is the distance between each sequenced nodes.

Subsequently the change in curvature between two sets of mode vectors i.e. the control and damaged cases is as shown in Eq. (2);

$$\text{CDF} = \frac{1}{N}\sum_{j=1}^{N}|C_{ci} - C_{di}| \quad (2)$$

where, CDF is the Curvature Damage Factor, N is the total number of modes, ‘c’ indicates control case when no load was applied and ‘d’ indicates damage case when damage load was applied and released and C is the curvature at ith node.

Figs. 4 and 5 show the results of CDF according to finite element modelling results with 50% of ultimate load (UL) applied at 550 mm and 1100 mm from the left support. Correspondingly the values of CDF with 70% of ultimate load applied to the beam at the same locations are illustrated in Figs. 6 and 7. The results were summated for the first six bending modes.

The results show that the CDF correlated well when the damage location was at 550 mm from left support for different degree of damage and it is apparent in Figs. 5 and 7 and match up to the crack pattern shown in Figure 3(b) and (d). However, when the damage was at mid-span it was less sensitive. Furthermore, values of CDF in all the cases considered, returned high values at the supports which is an anomaly and indicates a flaw in the algorithm. Thus, CDF in its original form is rather unreliable near the supports.

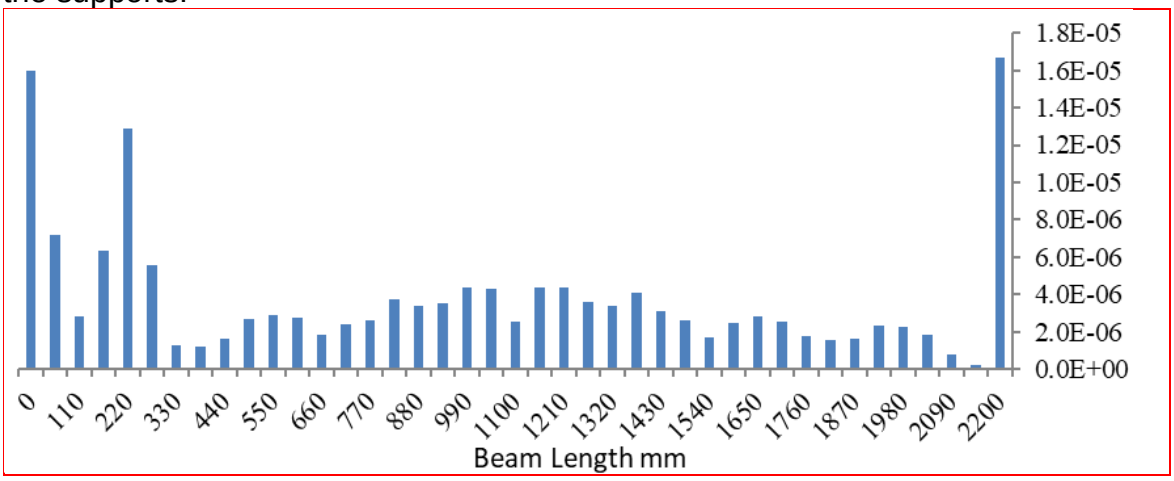

Fig. 4 CDF for beam under 50% UL (23 kN) located 1100mm from left support

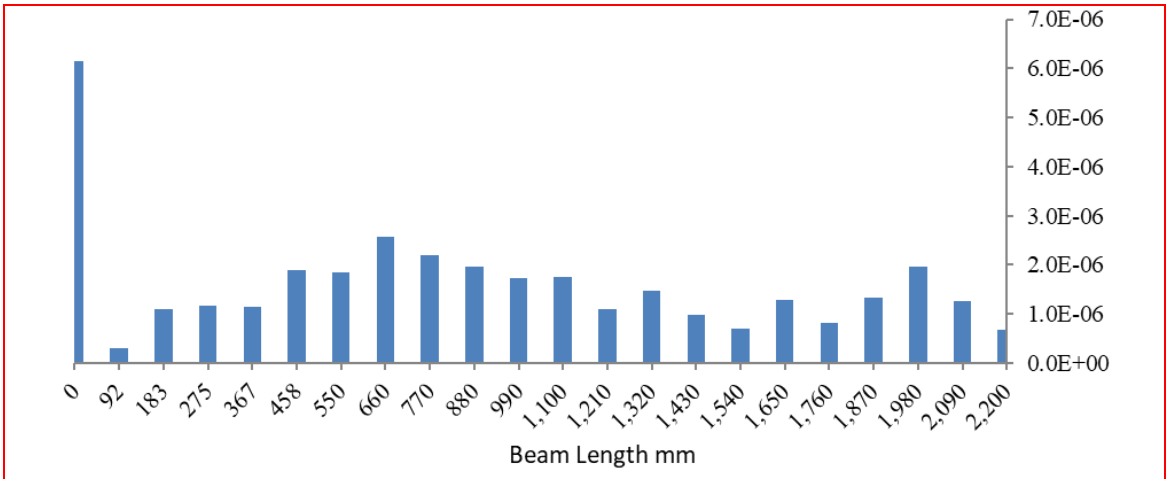

Fig. 5 CDF for beam under 50% UL (28 kN) located 550 mm from left support

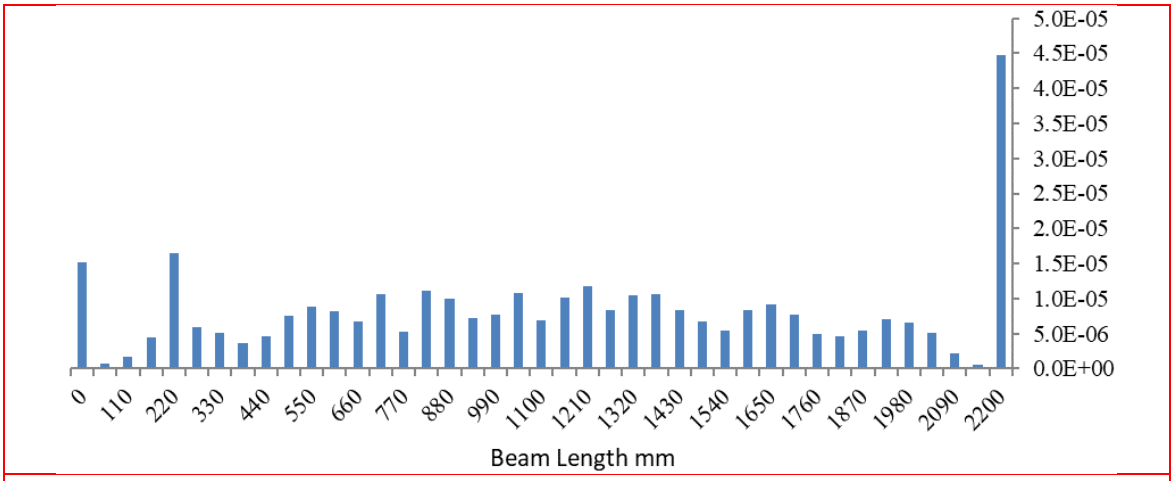

Fig. 6 CDF for beam under 70% UL (32.2 kN) located 1100 mm from left support

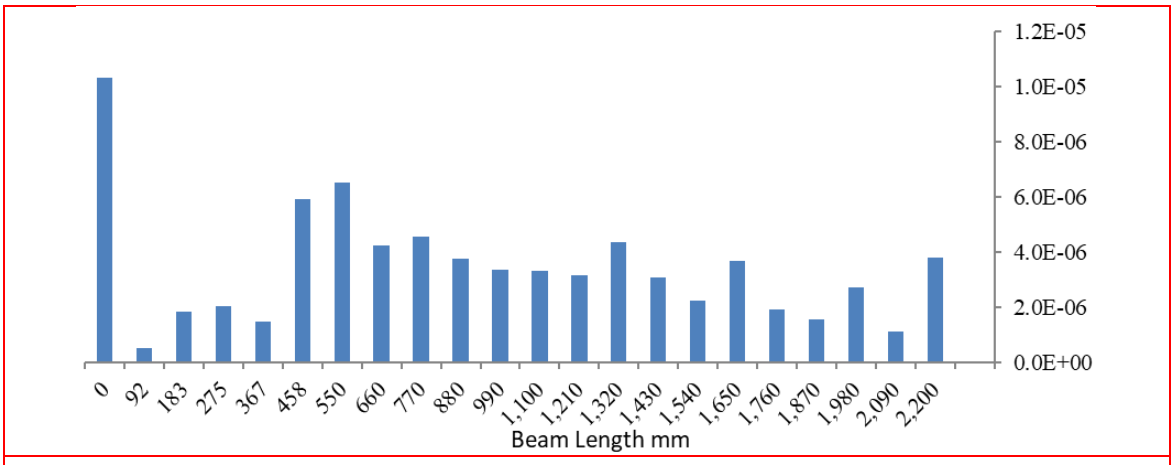

Fig. 7 CDF for beam under 70% UL (39.2 kN) located 550 mm from left support

3.2 Local Stiffness Indicator LSI

Proposed by Ismail and Abdul Razak (2006), it is based on the equation for free vibration of the Euler beam as shown below.

$$\frac{d^4y}{dx^2} - \lambda^4 \, y = 0 \tag{3}$$

Re-arranging the above equation in the following form;

$$\lambda^4 = \left|\frac{y^4}{y}\right| \tag{4}$$

In addition, applying the fourth order centered finite difference,

$$y^4 = (y_{i+2} - 4y_{i+1} + 6y_i - 4y_{i-1} + y_{i-2})/h^4 \tag{5}$$

where y^4 is the fourth derivative.

Thus, the Local Stiffness Indicator is defined as,

$$LSI = \lambda^4 \tag{6}$$

The solutions to Eqs. 3 and 6 when the node is located at the supports require special consideration. In this case, for a simply supported beam there is angle of rotation at the support which implies the line of elastic deformation which has the shape of the jth mode shape will pass through the support node to the next span and has the same angle of slope. Thus, the elastic deformation line will have the same shape but having opposite curvature. Fig. 8 shows the assumption of for the support node case. Subsequently, yi-1 = - yi+1 and yi-2 = - yi+2. The same assumption can be used at the other support,

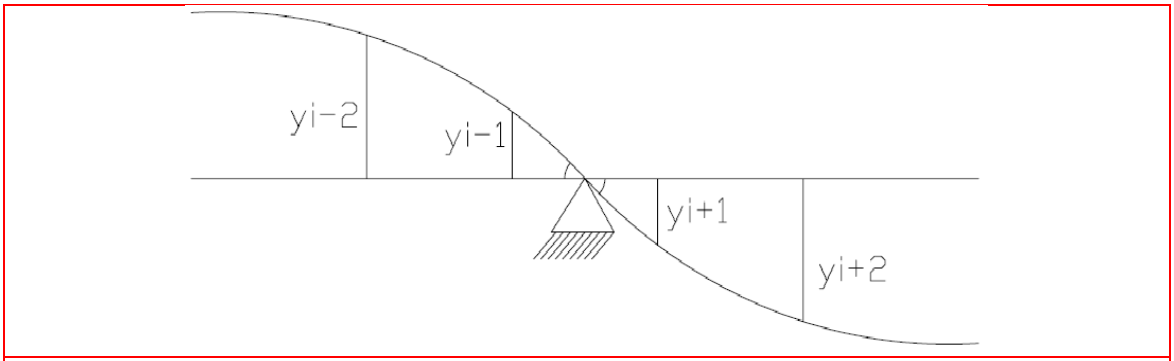

Fig. 8 Special consideration at support

The eigenvectors from the finite element model were extracted and substituted into the above equations to determine the LSI at each node. The occurrence of damage in the beam will cause a change in the LSI value at the damage location as compared to the undamaged beam where the values should remain constant throughout its length. Figs. 9 &10 depict the values of LSI for the finite element RC beam model with 50% of ultimate load applied at two different positions i.e. 550 mm and 1100 mm from left support. Figs. 11 &12 show the value of LSI for the finite element RC beam model with 70% of ultimate load applied at two different positions i.e. 550 mm and 1100 mm from the left support.

Apparently, the LSI is a less sensitive damage indicator compared to the CDF for damage location in the regions considered. However, the sensitivity is better at higher modes, and this can be observed when the damage is located at 0.25L by eliminating the support anomalies for modes 1,4,5 and 6 and subsequently reflects the ability to detect damage as shown in Figs. 10 and12. For regions at the support the values appear as anomalies and this is the major drawback of LSI indicator in its original form.

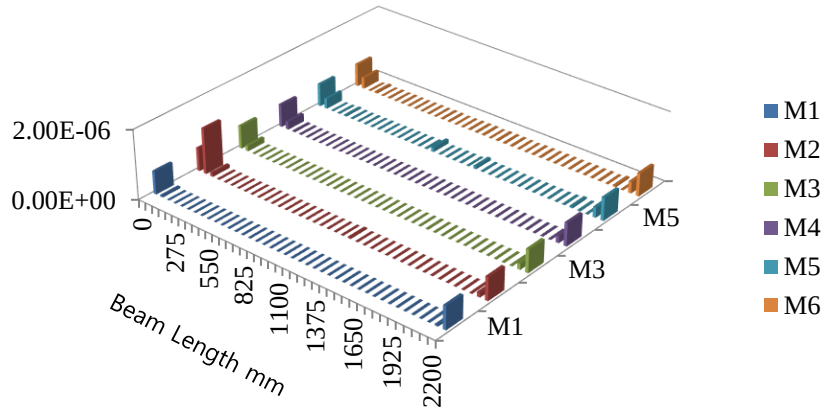

Fig. 9 LSI for beam under 50% UL (23kN) located at 1100 mm from left support, for mode shapes M1 to M6

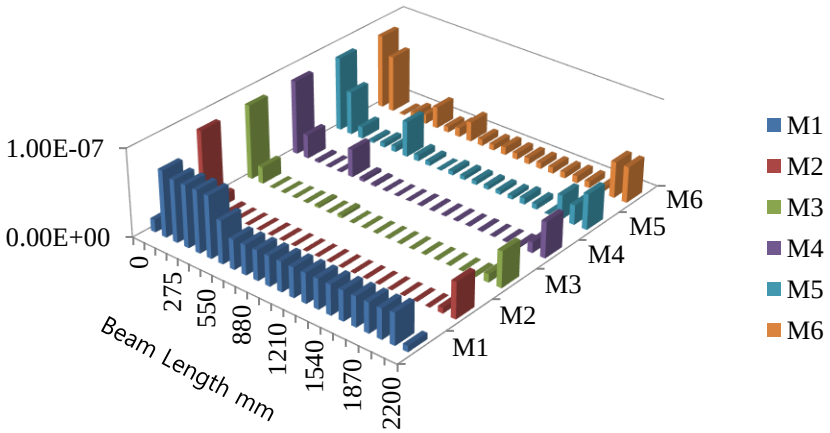

Fig. 10 LSI for beam under 50% UL (28 kN) located at 550 mm from left support, for mode shapes M1 to M6

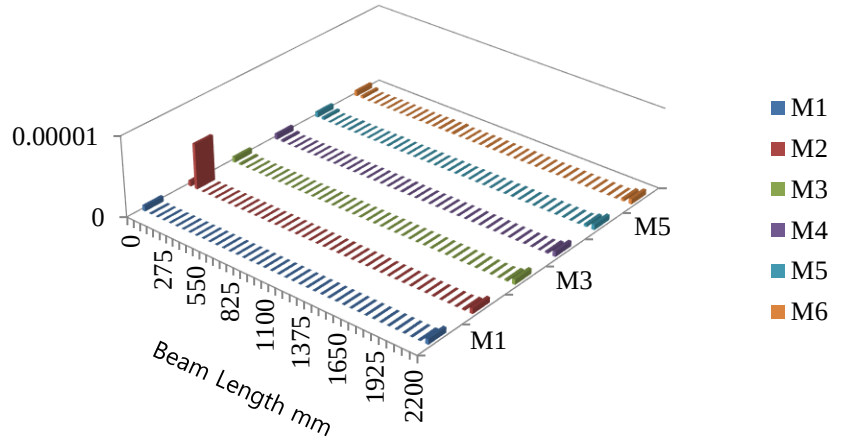

Fig. 11 LSI for beam under 70% UL (32.2 kN) located at 1100 mm from left support, for mode shapes M1 to M6

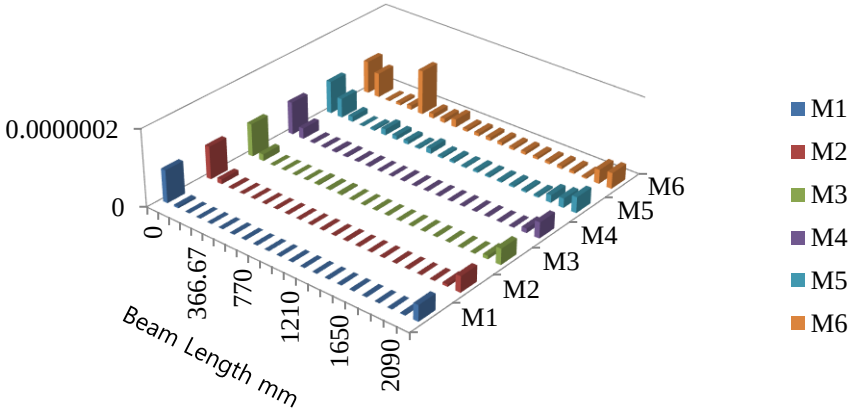

Fig. 12 LSI for beam under 70% UL (39.2 kN) located at 550 mm from left support, for mode shapes M1 to M6

4. Conclusions

From this study, the following conclusions can be drawn:

- Change in mode shape curvature correlated well when the damage location was at 550 mm from left support for different degree of damage. However, when the damage was at mid-span it was less sensitive.
- Values of mode shape curvature-based index in all considered cases returned high values at the supports which is an anomaly and indicates a flaw in the algorithm.
- The fourth derivative based index is a less sensitive damage indicator compared to the curvature-based index for damage location in the regions considered.
- The sensitivity of the fourth derivative based index is better at higher modes, and this can be observed when the damage is located at 0.25L by eliminating the support anomalies for modes 1,4,5 and 6.

Acknowledgments

The authors would like to acknowledge the financial assistance provided by University of Malaya. The authors would also like to thank all the people who have contributed in

any way to making this research possible.

References

ACI 318-08 (2008), *Building Code Requirements for Structural Concern,* American Concrete Institute, Farmington Hills, MI, USA.

Dutta, A., and Talukdar, S. (2004), "Damage Detection in Bridges Using Accurate Modal Parameters", *Finite Element in Analysis and Design,* **40**(3), 287-304. https://doi.org/10.1016/S0168-874X(02)00227-5.

Fayyadh, M.M., and Razak H.A. (2013), "Damage Identification and Assessment in RC Structures Using Vibration Data: A Review", *Journal of Civil Engineering and Management*, **19**(3), 375-386. https://doi.org/10.3846/13923730.2012.744773.

Fayyadh, M.M., and Razak, H.A. (2012), "Condition Assessment of Elastic Bearing Supports Using Vibration Data", *Construction and Building Materials*, **30**,616-628. https://doi.org/10.1016/j.conbuildmat.2011.12.043.

Fayyadh, M.M., Razak, H.A., Khaleel, O.R. (2011), "Differential Effects of Support Conditions on Dynamic Parameters", *Procedia Engineering*, **14**,177-184. https://doi.org/10.1016/j.proeng.2011.07.021.

Frans, R., Arfiadi, Y., and Parung, H. (2017), "Comparative Study of Mode Shapes Curvature and Damage Locating Vector Methods for Damage Detection of Structures", *Procedia Engineering*, **171**, 1263-1271. https://doi.org/10.1016/j.proeng.2017.01.420.

Ismail, Z., and Abdul Razak, H. (2006), "Determination of Damage Location In R.C. Beams Using Mode Shape Derivatives", *Engineering Structures*,**28**(11), 1566 -1573. https://doi.org/10.1016/j.engstruct.2006.02.010.

Pandey, A.K., Biswas, M., and Samman, M.M. (1991), " Damage Detection from Change in Curvature Mode Shapes", *Journal of Sound and Vibration*, **145**(2), 321-332. https://doi.org/10.1016/0022-460X(91)90595-B.

Pholdee, N., and Bureerat, S. (2016), "Structural health monitoring through meta-heuristics - comparative performance study", *Advances in Computational Design*, **1**(4), 315-327. DOI: http://dx.doi.org/10.12989/acd.2016.1.4.315.

Ratcliffe, C.P. (1997), "Damage Detection Using A Modified Laplacian Operator On Mode Shape Data", *Journal of Sound and Vibration*, **204**(3), 505 – 517. https://doi.org/10.1006/jsvi.1997.0961.

Razak, H.A., and Fayyadh, M.M. (2013), "Sensitivity of Natural Frequencies to Composite Effects in Reinforced Concrete Elements", *Mechanics of Advanced Materials and Structures*, **20**(6),441-453. https://doi.org/10.1080/15376494.2011.627636.

Shokrani, Y., Dertimanis, V.K., Chatzi, E.N., and Savoia, M.N. (2018), "On The Use of Mode Shape Curvature for Damage Localization Under Varying Environmental Conditions", *Structural Control Health Monitoring*, **25**(4), e2132. https://doi.org/10.1002/stc.2132 .

Stubbs, N., Kim J.T., and Farrar C.R. (1995), "Field Verification of Non Destructive Damage Localization and Severity Estimation Algorithm", *Processing of the 13th international modal analysis conference,* Tennessee, USA, February.

Wahab, M.M.A., and De Roeck G. (1999), "Damage Detection in Bridges Using Modal curvature: Application to A Real Damage Scenario", *Journal of Sound and Vibration*, **226**(2), 217-235. https://doi.org/10.1006/jsvi.1999.2295.